RESEARCH ARTICLE

Macromolecular Rapid Communications
www.mrc-journal.de

End-To-End FRET Enabling Direct Measurement of Oligomer Chain Conformations and Molecular Weight in Reaction Solutions

*Sara Valdez, Syba Ismail, Yuming Wang, and Zhe Qiang**

Förster resonance energy transfer (FRET) is an established tool for measuring distances between two molecules (donor and acceptor) on the nanometer scale. In the field of polymer science, the use of FRET to measure polymer end-to-end distances (R_{ee}) often requires complex synthetic steps to label the chain ends with the FRET pair. This work reports an anthracene-functionalized chain-transfer agent for reversible addition-fragmentation chain-transfer (RAFT) polymerization, enabling the synthesized chains to be directly end-labeled with a donor and acceptor without the need for any post-polymerization functionalization. Noteworthily, this FRET method allows for chain conformation measurements of low molecular weight oligomers in situ, without any work-up steps. Using FRET to directly measure the average R_{ee} of the oligomer chains during polymerization, the chain growth of methyl methacrylate, styrene, and methyl acrylate is investigated as a function of reaction time, including determining their degree of polymerization (*DP*). It is found that *DP* results from FRET are consistent with other established measurement methods, such as nuclear magnetic resonance (NMR) spectroscopy. Altogether, this work presents a broadly applicable and straightforward method to in situ characterize R_{ee} of low molecular weight oligomers and their *DP* during reaction.

1. Introduction

The chain conformation of polymer materials significantly impacts their macroscopic properties, such as mechanical strength and electrconductivity, as these properties are influenced by the spatial behavior and interactions of the polymer chains (e.g., chain entanglements).[1,2] Specifically, altering chain conformation provides a route to modulate material properties, which can be achieved through kinetically trapping polymer chains in non-equilibrium states.[3–7] Understanding the process-structure-property relationship is a central interest in the polymer community. Therefore, characterizing chain conformations is fundamentally important for controlling polymer properties and designing materials for various applications including soft robotics,[8] filtration membranes,[9] and microelectronics.[10]

Current methods to measure chain conformation commonly rely on scattering-based techniques, including optical light,[11] X-ray,[12,13] and neutron scattering.[14–17] Both X-ray and neutron scattering techniques provide reciprocal space data over a relatively large sample volume. With model fitting, several physical parameters of single chain behaviors such as persistence length and contour length can be obtained. Additionally, through measuring the light scattering intensity as a function of polymer concentration, Zimm analysis can be used to extrapolate polymer molecular weight and chain dimensions.[1] While these methods can give information about the radius of gyration (R_g), generally, the end-to-end distance (R_{ee}) is much more difficult to measure experimentally. Additionally, most investigations of chain conformation focus on relatively high molecular weight systems (greater than ≈10, 000 Da) due to the increased difficulty of obtaining an adequate scattering signal for chains with smaller dimensions (e.g., R_g~1 nm). In 2020, Sherck et al. reported a method to address this challenge by using double electron-electron resonance (DEER) spectroscopy to measure R_{ee} of low molecular weight polymers, using poly(ethylene oxide) (PEO) as a model system.[18] Specifically, DEER is a pulsed paramagnetic resonance technique that is able to measure the mean distance as well as the distance distribution between two spin probes on the scale of ≈2–9 nm.[19,20] By labeling the chain ends with the spin probes, the R_{ee} and distance distributions of PEO can be obtained over a molecular weight range of 0.22–2.6 kDa.

Alternatively, Förster resonance energy transfer (FRET) is an established method to measure distances between a FRET pair (donor and acceptor molecules) when they are in the range of ≈1–10 nm.[21,22] This method has often been employed in biological systems to elucidate detailed molecular-level behaviors, such as protein folding,[23–25] metabolic events,[26,27] and

S. Valdez, Y. Wang, Z. Qiang
School of Polymer Science and Engineering
The University of Southern Mississippi
118 College Drive, Hattiesburg, MS 39406, USA
E-mail: zhe.qiang@usm.edu
S. Ismail
Department of Chemistry
Chatham University
107 Woodland Rd, Pittsburgh, PA 15232, USA

DOI: 10.1002/marc.202400627

cell membrane interactions.[28–30] FRET is a distance-dependent process, based on a Coulombic interaction through resonance where energy is transferred non-radiatively from the excited-state donor to an acceptor. The change in the energy transfer efficiency is related with the distance between the FRET pair. Several key requirements for FRET to occur include: 1) there must be sufficient overlap between the donor's emission and acceptor's absorbance spectra and 2) the donor and acceptor need to be in close proximity (≈1–10 nm). It is important to note that the acceptor molecule may, but does not have to, be fluorescent. Noteworthily, FRET is still underutilized in synthetic polymer systems, with most work leveraging it to determine polymer micelle formation,[31–33] interfacial behaviors of polymeric systems,[34,35] and polymer chain dynamics[36–38]; their use to characterize quantitative polymer chain conformation is still limited.[39] Sha et al. used intermolecular FRET to measure the R_{ee}s of poly(methyl methacrylate) (PMMA) and polystyrene (PS) end-labeled with anthracene and carbazole synthesized by atom-transfer radical polymerization (ATRP) and azide-alkyne click chemistry.[40,41] Moreover, Qin et al., investigated how polymer solution concentrations impact chain conformation transitions.[39,42] However, for these systems, a multistep synthetic approach and extensive purification is necessary for labeling chains with the FRET pair, which can be time consuming and difficult to achieve a 1:1 donor-to-acceptor ratio.

Furthermore, directly measuring the size of molecules in crude solutions during chemical reactions is difficult due to the very limited techniques available, which require high measurement sensitivity and accuracy. The complexity of these measurements is often compounded by the dynamic nature of the reaction environment such as low and varied sample concentrations as a function of reaction time. To address this significant challenge, a FRET-based method is developed in this work to directly quantify oligomer chain R_{ee} in a crude solution without additional sample workup including drying and purification, leveraging the advantages of fluorescence measurements which offer high sensitivity.[43–46] Our in situ method is enabled by the use of reversible addition-fragmentation chain-transfer (RAFT) polymerization, which can prepare polymers with controlled molecular weight, low molecular weight dispersity ($Đ$), and defined end-groups with high fidelity, facilitated by use of the chain-transfer agent (CTA). Moreover, many RAFT CTAs can absorb light in the UV range due to a π-π^* transition and a forbidden n-π^* transition[47] which can conveniently be leveraged to quench the emission of fluorophores that are sufficiently close.[48] Specifically, α,ω-hetertotelechelic oligomers of methyl methacrylate (MMA), styrene (S), and methyl acrylate (MA) end-capped with anthracene (donor) and dithiobenzoate (acceptor) are prepared, to investigate their chain conformation during polymerization in a good solvent (toluene). The presence of dithiobenzoate (CTA) molecules can quench anthracene emission, allowing the two molecules to act as a FRET pair. Using this reported system, we are able to streamline the functional material synthesis containing a FRET pair, enabling direct R_{ee} and DP measurements during the reaction without purification steps and can be broadly applicable to other oligomer systems.

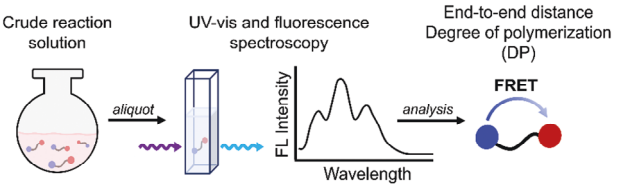

Scheme 1. Scheme of procedure to measure chain conformations and DPs of oligomers using fluorescence emission intensities of crude reaction solutions of chains end-labeled with a FRET pair (donor and acceptor).

2. Results and Discussion

In this work, we use a rationally designed fluorescent CTA in conjunction with RAFT polymerization. This method directly produces oligomer chains end-capped with a FRET pair, enabling potential in situ quantitative characterization of their R_{ee} and DP while still in the crude reaction mixture (Scheme 1). Specifically, the FRET efficiency can first be determined by fluorescence spectroscopy measurements and then be correlated with the distance between donor and acceptor molecules. When these molecules are attached to the respective ends of an oligomer or polymer chain, this measurement can directly report the chain's R_{ee}. This approach can provide a significantly more streamlined technique for obtaining accurate and reliable information about chain conformation and sample molecular weight.

Anthracene was used as the FRET donor and the dithiobenzoate group of 4-cyano-4-(phenyl-carbonothioylthio)pentanoic acid (CPTP) acted as the acceptor. We note that by first coupling the CPTP with the donor, a simple synthetic route can be developed to prepare oligomers end-labeled with the FRET pair that would not require any post-polymerization reactions or further purification to measure the chain conformation. Particularly, this method takes advantage of the high end-group fidelity of RAFT polymerization facilitated by the CTA, resulting in the synthesis of D, A-end labeled oligomers. To prepare the FRET-pair containing CTA, the CPTP molecule was first reacted with 9-anthracenemethanol (AnOH) via a Steglich esterification reaction, resulting in CPTP-An. As shown in **Figure 1a**, all peaks from the ^{1}H NMR spectrum of CPTP-An can be assigned to their corresponding protons. Specifically, the shifting of the methylene peak α to the aromatic group (peak g in Figure 1a) from 5.67 to 6.21 ppm indicates the successful esterification between CPTP and AnOH molecules. Mass spectrometry and ^{13}C NMR spectroscopy were also performed with CPTP-An to further confirm the successful esterification (results shown in Figures S1 and S2, Supporting Information, respectively).

To provide a brief background, FRET is a non-radiative energy transfer process that occurs between an excited donor and an acceptor in close proximity (1–10 nm), as illustrated in Figure 1b. For this transfer to occur, a key requirement is sufficient overlap between the donor's emission spectrum and the acceptor's absorption spectrum; the acceptor itself does not need to be emissive. Additionally, the distance range that can be measured by a specific FRET pair is associated with its Förster distance (R_o, defined quantitatively in Equation 3 in the Experimental Section). R_o is also defined as the distance between the donor and acceptor

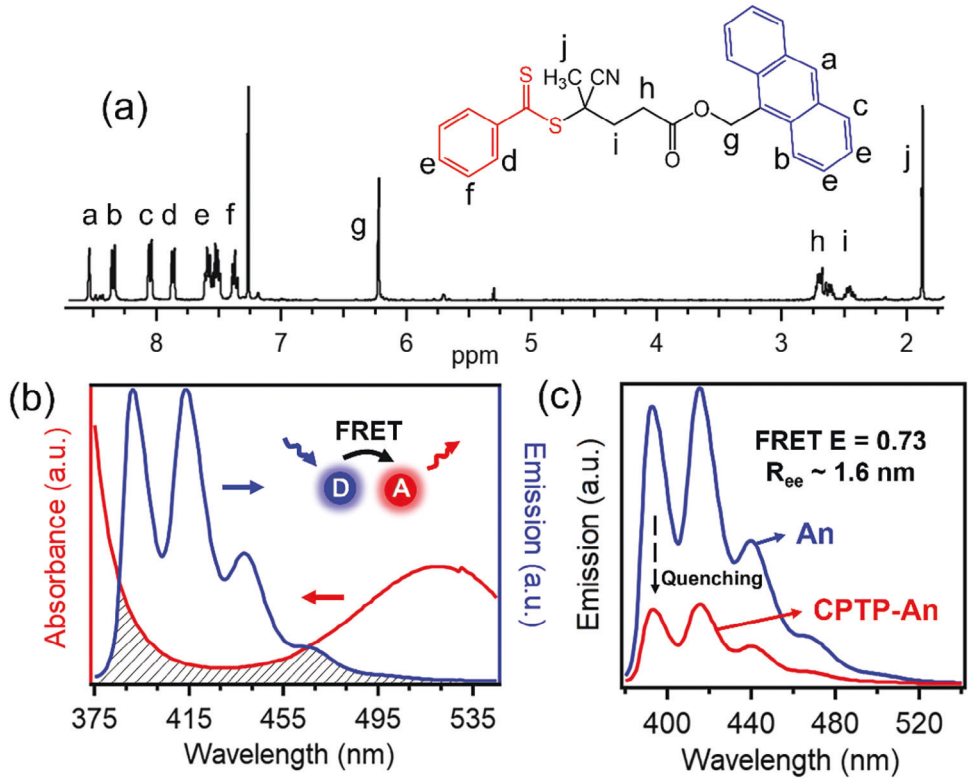

Figure 1. a) Labeled ^{1}H NMR spectrum of CPTP-An (in $CDCl_3$-7.26 ppm), which can be used as the FRET pair-labeled CTA (donor is shown in blue and the acceptor in red), b) absorption spectrum of CPTP (red) and emission spectrum of anthracene (blue) with an excitation wavelength of 365 nm, and c) An and CPTP-An emission using an excitation wavelength of 365 nm and measured over a wavelength range of 380–540 nm, illustrating anthracene emission quenching caused by CPTP when it is in close proximity to An, and the FRET efficiency of the CTA is 73%, corresponding to a R_{ee} of ≈1.6 nm.

when the FRET efficiency, *E*, is 50%. It was determined that the R_o for CPTP-An was ≈1.85 nm and additional details of the R_o calculation can be found in the Experimental Section using Equation 5. Figure 1b shows the fluorescence emission spectrum of AnOH excited at 365 nm and the absorption spectrum of CPTP in the range of 380–540 nm. We note that while multiple approaches are available to determine the FRET efficiency, such as donor or acceptor photobleaching and acceptor sensitization,[49] this work focused on monitoring the donor emission intensity in the presence and absence of acceptor molecules, respectively, as described in Equation 5 in the Experimental Section. The distance between respective ends of CPTP-An was first measured. As shown in Figure 1c, when the anthracene molecule is chemically attached to CPTP, the fluorescence emission intensity significantly decreases due to the quenching effect from the presence of the dithiobenzoate group, leading to a FRET efficiency of 73%, corresponding to a R_{ee} of ≈1.6 nm for CPTP-An which is very similar to the distance calculated for CPTP-An using bond lengths/angles (≈1.64 nm).

In our previous work,[53] CPTP-An was used to prepare polymers end-labeled with donor and acceptor molecules, allowing FRET measurements to determine their molecular size, specifically R_{ee} . While this work uses the same CTA, an additional level of sophistication was introduced to directly address a key bottleneck in the in-situ characterization of polymerization kinetics. This bottleneck is associated with the lack of measurement tools to quantify molecular weight in crude reaction solutions. Specifically, we employed the as-synthesized CPTP-An to perform RAFT polymerization and took measurements directly from crude reaction solutions, enabling streamlined characterization of chain conformation and molecular weights. This method provides significant advantages for further opportunities of in situ characterization of chain size and *DP* during the reaction through fluorescence-based characterization measurements. **Figure** 2a illustrates the RAFT polymerization of our model system where methyl methacrylate (MMA) is used as the monomer to directly produce oligomers labeled with a FRET pair. The reaction was performed at 75 °C, with a target molecular weight (*MW*) of 10,000 Da (corresponding to a *DP* of 100) and an initial monomer concentration of 1.5 M. For this study, aliquots were taken throughout the polymerization to monitor changes in chain conformation and *DP* as the reaction progressed (0 to 135 min). ^{1}H NMR spectroscopy measurements were used to monitor reaction progress using end-group analysis to determine the *DP* of different oligomeric samples, as shown in Figure 2b. Specifically, the end-group analysis was performed by monitoring the area of the highlighted peaks corresponding to the repeating unit (MMA, methyl ester peak at 3.6 ppm, *3H*) and the anthracene (aromatic peak at 8.5 ppm, *1H*) end group from the CTA. By increasing the reaction time, the relative peak intensity of the methyl ester peak corresponding to MMA increases from 0 to 16.3 (*DP* of 5.4) after 45 min, 22.3 (*DP* of 7.4) after 60 min, 45.2 (*DP* of 15) after 85 min, and 65.0 (*DP* of 22) after 135 min, attributed to the chain growth of repeating units inserted on the

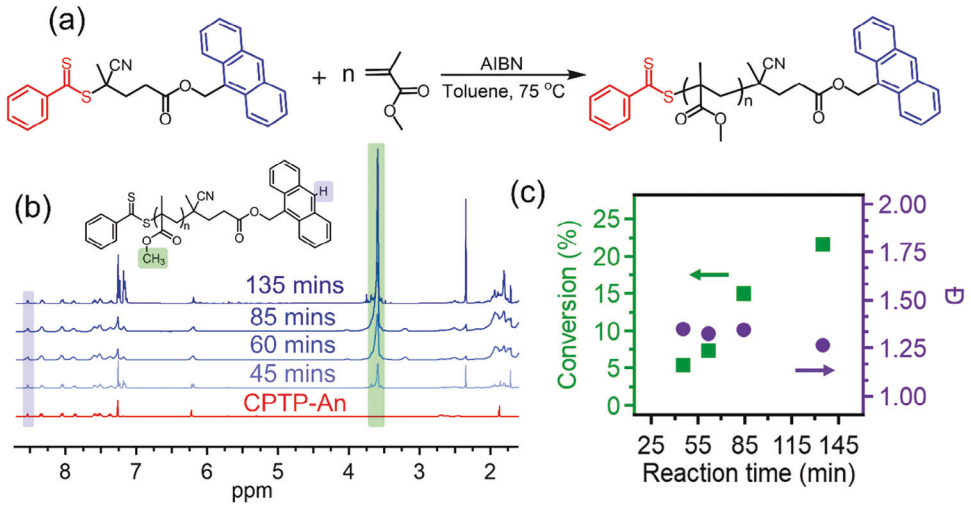

Figure 2. a) RAFT polymerization of MMA using CPTP-An as the CTA, b) ^{1}H NMR spectra of aliquots taken during the reaction with end-group analysis peaks highlighted (end-group proton highlighted with blue and monomer protons with green), and c) reaction conversion (green squares, left axis, determined using DP from NMR analysis and the target DP) and Đ (purple circles, right axis, determined by GPC analysis) as a function of reaction time throughout the MMA polymerization.

backbone of CTA. These results were then compared with the target *DP* to calculate reaction conversion, as shown in Figure 2c. The reaction conversion increased from ≈5 to 22% as a function of increasing reaction time from 45 to 135 min, which in general follows a linear trend. This linear trend is indicative of a living polymerization, a characteristic of controlled polymerization. In addition to determining the *DP* and conversion of the oligomer MMA (oligoMMA) samples, the ^{1}H NMR spectra also show that the entire CPTP-An fragment is still present on the synthesized chains. For each reaction time point, the ratio of the integrations of CPTP-An peak a (anthracene, *1H*) to d (dithiobenzoate, *2H*) (Figure 1a) remains 1:2, indicating that the FRET D:A ratio remains very close to 1:1 throughout the polymerization reaction in this work. This feature is important as stoichiometric labeling efficiency is imperative for quantitative FRET measurements; a high concentration of chains with only a donor could lead to challenges in obtaining accurate FRET efficiencies. Gel permeation chromatography (GPC) was performed to monitor *Đ* throughout the reaction for different samples, shown in Figure 2c and Figure S3 (Supporting Information). The dispersity slightly decreased from 1.35 to 1.26 from 45 min to the end of the reaction (135 min), suggesting that more control was established as the reaction progressed and molecular weight increased, which is consistent with other groups of RAFT polymerization.[50–52]

Fluorescence spectroscopy measurements were then performed on the oligoMMA aliquots using an excitation wavelength of 365 nm and collected over the range of 380–540 nm. All emission intensities were normalized to the molar concentration of anthracene measured by UV-vis spectroscopy using anthracene's molar absorptivity, 8528 L mol^{-1} cm^{-1} at 365 nm (**Figure 3a**). This normalization allows for a direct comparison of the change in anthracene emission intensity as a function of reaction time. The intensities of all of the aliquots from the crude reaction fall between anthracene and CPTP-An. Specifically, as the reaction time increased, the emission intensity of anthracene became stronger, indicating that less quenching (energy transfer) had occurred from the presence of the dithiobenzoate while retaining the same characteristic shape of anthracene emission (three distinct peaks at 393, 415, and 439 nm). This phenomenon is anticipated because as the chains grow and more repeat units are inserted between the CTA end groups, the donor and acceptor molecules move further apart. This increased distance leads to decreased energy transfer efficiency, which experimentally appears as an increased emission intensity of anthracene. We would like to note that while this distance measurement technique primarily relies on FRET, the emission intensity of anthracene can also be potentially decreased through other processes including scattering, photobleaching (during synthesis, storage, or measurement), UV absorption of other oligomer chains, and changes to anthracene's electronic environment after being attached to the CTA. Moreover, to obtain more quantitative information, the FRET efficiencies were calculated using the ratio of the normalized emission intensities of the oligomer chains to neat anthracene (equation 5 in Experimental Section). As revealed by the concentration normalized emission spectra, FRET efficiencies continued to decrease as the reaction progressed (Figure 3b). The efficiencies decreased from 73% at time zero (obtained from just CPTP-An) down to 41, 31, 18, and 10% after 45, 60, 85, and 135 min, respectively. From these results, we can then determine the average R_{ee} of oligomer chains using the FRET efficiency value of aliquot samples and the R_o of CPTP-An (1.85 nm); our calculation (Equation 7 in the Experimental Section) considers the flexible chain model to describe chain size distribution (Figure S4, Supporting Information). The calculated averaged R_{ee} distances are shown in Figure 3c where with increasing reaction time, the average distance increased from 1.6 nm at time zero to 2.4 nm at 45 min, 2.8 nm at 60 min, 3.6 nm at 85 min, and 4.6 nm after 135 min.

To further assess the quantitative validity of the chain conformation measurements obtained with FRET, the measured values were compared with results from all-atom molecular dynamics (MD) simulation of PMMA from a previous

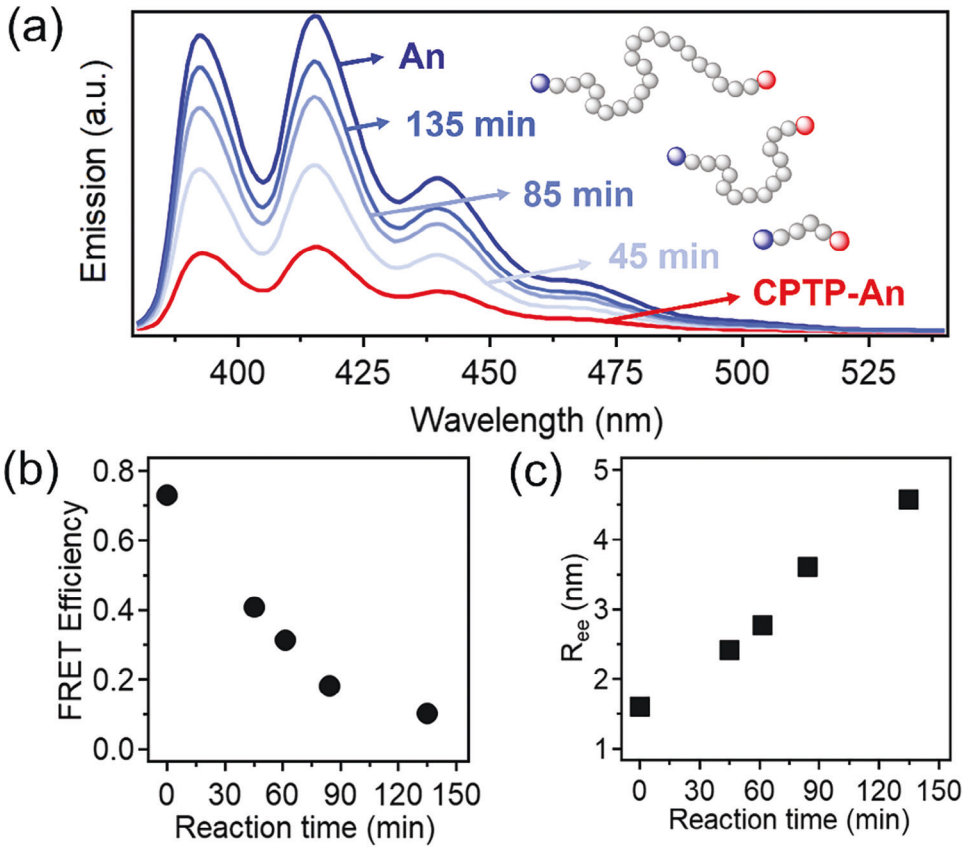

Figure 3. a) Molar-concentration normalized fluorescence emission intensities of CPTP-An and oligoMMA molecules throughout the reaction with an excitation wavelength of 365 nm, b) FRET efficiency as a function of the MMA polymerization reaction time, and c) their corresponding R_{ee} as a function of reaction time.

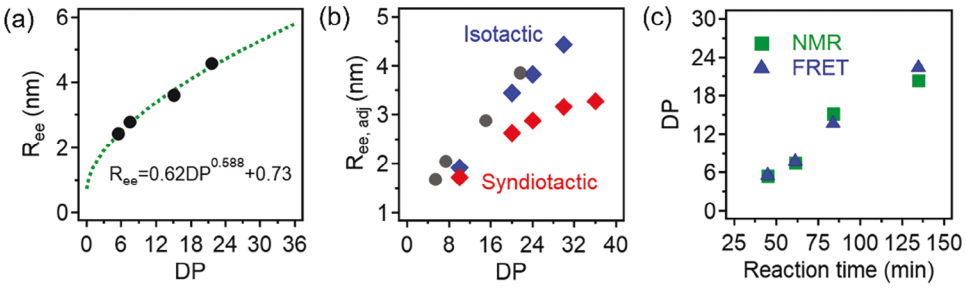

Figure 4. a) Plot of FRET measured R_{ee}s against DP (from NMR) of oligoMMA samples, and the green trace is the fit function, $R_{ee} = 0.62DP^{0.588}+0.73$, b) plot of $R_{ee,adj}$ ($R_{ee,adj} = R_{ee}$-0.73) against DP (from NMR) compared to simulated R_{ee}s of isotactic (blue diamonds) and syndiotactic (red diamonds) PMMA, and c) DP determined by FRET (blue triangles) and NMR (green squares) during the MMA polymerization.

study;[53] we note that the simulation data account for either isotactic or syndiotactic conformations but do not include chain ends. Therefore, to directly compare the R_{ee} values, the contribution of the CTA chain ends to the measured R_{ee}s needs to be accounted for. As shown in **Figure** 4a, the measured R_{ee}s were plotted against the *DP*s determined by NMR end-group analysis, and the data points were fitted to the following equation:

$$R_{ee} = a(DP)^{v} + b, \quad (1)$$

where *a* is a coefficient related to monomer chemistry, *b* is a factor that influences polymer R_{ee} accounting for the presence of end groups, as well as other factors such as polydispersity and end-group fidelity. It is important to note that the *b* value is purely a result of fitting parameters and does not have a distinct physical meaning, and *v* is a scaling exponent that is dependent on solvent solubility (held at 0.588 as these samples are oligomer chains in a good solvent). Upon fitting, the resulting equation for oligoMMA was found to be $R_{ee} = 0.62DP^{0.588}+0.73$. We note that this *b* value is only about half of the length of CPTP-An (1.6 nm), and it was

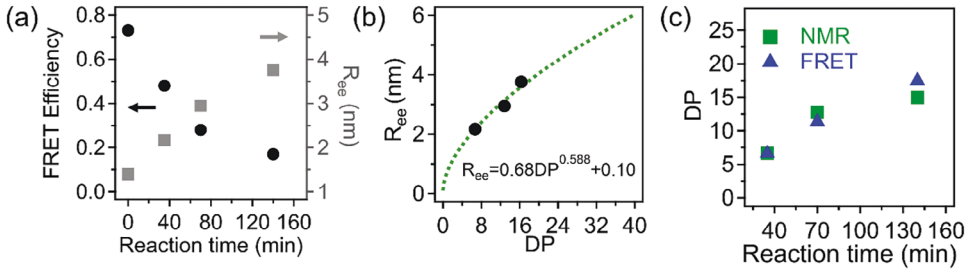

Figure 5. a) FRET efficiency (black circles) and their corresponding R_{ee}s (grey squares) as a function of styrene polymerization reaction time, b) plot of FRET measured R_{ee}s against DP (from NMR) of oligoS samples, the green trace is the fit function, $R_{ee} = 0.68DP^{0.588}+0.10$, and c) DP determined by FRET (blue triangles) and NMR (green squares) during the styrene polymerization.

anticipated that the fitted parameter be less than 1.6 nm (and positive) since the 1.6 nm is the CTA in a fully extended conformation but once monomers begin to be inserted, the chain may start to become coil-like in a good solvent. Additionally, this value is an approximation of the contributions from multiple factors including end group, polymerization conditions, molecular weight distribution, etc. Using the information from the fit equation, an adjusted R_{ee}, defined as $R_{ee,\,adj}$, was able to be determined by subtracting 0.73 nm (b from the power law fit) from the R_{ee}s measured by FRET. The $R_{ee,\,adj}$ was then compared to the simulated values shown in Figure 4b. We note that the synthesized oligomers are atactic as the tacticity was not controlled during our RAFT polymerization. The adjusted FRET-measured R_{ee} of all samples is close to the simulation results of isotactic counterparts at the same molecular weights, suggesting the accuracy of our streamlined FRET measurement method. The quantitative R_{ee} difference, even though generally less than 1 nm, can be attributed to the polydispersity of the resulting oligomer samples as well as the potential resolution limits of the FRET measurements. Furthermore, using the fit for the data and the measured distances of the oligoMMA samples, the *DP*s for each aliquot could be calculated from the FRET data. The averaged *DP*s determined from the FRET measurements increased from 5.5 to 7.6, 14, and 22 after 45, 60, 85, and 135 min, respectively. The FRET *DP*s are compared to the NMR *DP*s in Figure 4c. From this plot, an excellent agreement can be observed from *DP*s determined from NMR end-group analysis and FRET measurements. These results not only demonstrate that our FRET-based R_{ee} measurement method, derived from streamlined measurements of crude reaction solutions, is accurate, but also highlight its significant advantage in further enabling in situ, in-reaction characterizations. Additionally, our findings suggest the potential of using this method as an alternative approach for determining the *DP* of oligomers without requiring additional sample work-up and preparation.

To demonstrate the generalizability of this technique, we extended it to two additional monomer systems, including styrene (S) and methyl acrylate (MA), using the same FRET pair-labeled CTA, CPTP-An, and RAFT polymerization method. For styrene, the polymerization was done at 100 °C with a target *MW* of 10,000 (*DP* of ~100) with aliquots taken over 0–140 min. NMR end-group analysis results yielded *DP*s of 6.7, 13, and 16 for 35, 70, and 140 min, respectively (Figure S5, Supporting Information). GPC results showed that throughout the styrene polymerization, *Đ* decreased from 1.15 to 1.15, and 1.14 for reaction times of 35, 70, and 140 min, respectively, as shown in Figure S6 (Supporting Information). The GPC traces and reaction conversion results can be found in Figure S6 (Supporting Information). For the oligoS samples, the FRET efficiencies were calculated using the same method described for oligoMMA and are shown in **Figure 5a**. We observed an anticipated decrease in FRET efficiency as the reaction proceeded, where the efficiency started at 73% and decreased to 48% at 35 min, 28% at 70 min, and 17% at 140 min. The FRET efficiencies were then used to determine the average R_{ee}s of the chains, as shown in Figure 5a. The distances grew from 1.6 nm at time zero to 2.2, 3.0, and 3.8 nm at 35, 70, and 140 min, respectively. The p(R_{ee}) using Equation 7 (Experimental Section) considering the flexible chain model for oligoS can be found in Figure S7 (Supporting Information). In a similar manner as oligoMMA, the measured R_{ee}s were plotted against the *DP*s from NMR and fit to the same power law (Equation 1; Figure 5b) again with ν held at 0.588. This gave a fit equation of $R_{ee} = 0.68DP^{0.588}+0.10$. The $R_{ee,\,adj}$s were calculated by subtracting 0.10 nm from the measured R_{ee}s, so the $R_{ee,\,adj}$s could be directly compared to MD simulated R_{ee}s of isotactic and syndiotactic PS (Figure S8, Supporting Information). We observe less influence of the tacticity on the R_{ee}s of the simulated PS distances and the experimentally-measured R_{ee}s ($R_{ee,\,adj}$s) are slightly higher than the simulated but are still comparable to the distances at the same *DP*s. The FRET data could then be used to calculate the *DP* using the fit equation. The FRET calculated averaged *DP*s increased from 6.6 to 11, and 18 after 35, 70, and 140 mins, respectively. These results are compared to the NMR *DP*s in Figure 5c. The FRET results again align well with the NMR end-group analysis *DP*s, representative of a good fit of the R_{ee} data, further demonstrating the robustness of the synthetic method to measure chain conformations in crude reaction mixtures.

For MA, the reaction was run at 85 °C with a target *DP* of 125, and aliquots were taken over reaction times ranging from 0 to 205 min with an initial monomer concentration of 1.9 M; all of the results can be found in the Supporting Information. Specifically, ^{1}H NMR end-group analysis gave *DP*s of 3.4, 5.6, and 8.0 for 60, 120, and 205 mins, respectively (Figure S9, Supporting Information). The GPC traces, conversion, and *Đ* results can be found in Figure S10 (Supporting Information). As with oligoMMA and oligoS, as the reaction progressed the FRET efficiency decreased (73% at 0 min, 59% at 60 min, 45% at 120 min, and 18% at 205 min) and the R_{ee}s increased (1.6 nm at 0 min, 1.9 nm at 60 min, 2.3 nm at 120 min, and 3.6 nm at 205 min), as shown

in Figure S11 (Supporting Information). The p(R_{ee}) considering the flexible chain model for oligoMA can be found in Figure S12 (Supporting Information). Additionally, Figure S13 (Supporting Information) displays the measured R_{ee}s for all monomers in this study (MMA, S, and MA) showing that our measurements span the majority of the range measurable with this FRET pair-labeled CTA, CPTP-An. Collectively, these results confirm that our method can be extended to determine *DP* and R_{ee} for various monomer chemistries in RAFT polymerization.

3. Conclusion

In this work, we develop a facile platform to enable end group-labeled oligomer chains with a FRET pair to directly measure their R_{ee} and *DP* in a crude reaction solution. Specifically, an anthracene functionalized CTA is synthesized and utilized in RAFT polymerizations of MMA, MA, and styrene to produce donor, acceptor end-labeled chains that could be characterized without any post-polymerization reactions or further purification. Energy transfer efficiencies between anthracene and the dithiobenzoate group of the CTA of different samples can be measured in situ during their reactions by taking aliquots and monitoring their fluorescence emission intensities. These efficiencies could then be used to determine the chain dimensions in solution state. We confirm the accuracy of the measurements by comparing the R_{ee}s to all-atom molecular dynamic simulation results. The R_{ee}s is also used to calculate the *DP*s of the oligomeric samples, which show good agreement with results from NMR end-group analysis. Overall, this method allows for streamlined measurements of chain conformation and *DP* of short oligomer chains without a need for further reactions for dye labeling or purifications and can be further extended to other systems for enabling in situ characterization within crude reaction solutions.

4. Experimental Section

Materials: Methyl methacrylate (MMA, 99%), styrene (99%), methyl acrylate (MA, 99%), 4-(dimethylamino)pyridine (DMAP, 99%), N,N'-dicyclohexylcarbodiimde (DCC, 99%), 2,2′-Azobis(2-methylpropionitrile) (AIBN, 98%), and 4-cyano-4-(phenyl-carbonothioylthio)pentanoic acid (CPTP) were purchased from Sigma-Aldrich. Deuterated chloroform ($CDCl_3$, 99.6 atom %D) and 9-(hydroxymethyl)anthracene (AnOH, 98%) were purchased from TCI America. Methylene chloride (DCM, Certified ACS Reagent), toluene (Certified ACS Reagent), and hexanes (Certified ACS Reagent) were purchased from Fisher Chemical. Tetrahydrofuran UV (THF, HPLC grade) was purchased from Honeywell. MMA, styrene, and MA monomers were purified with basic aluminum oxide (Sigma-Aldrich) to remove inhibitors (4-methoxyphenol for MMA/MA and 4-tert-butylcatechol for styrene). All other chemicals were used as received.

Synthesis of Anthracene Functionalized CTA (CPTP-An): CPTP-An was synthesized via Steglich esterification. CPTP (600 mg, 2.1 mmol, 1 equiv.) and AnOH (895 mg, 4.3 mmol, 2 equiv.) were added to a 25 mL round bottom flask (RBF) with DCM to dissolve CPTP and AnOH (≈10 mL) and was left to stir over ice for 5 min. DMAP (446 mg, 3.7 mmol, 1.7 equiv.) dissolved in ≈1 mL of DCM was then added to the reaction mixture and left to stir for 10 min. DCC dissolved in ≈1 mL of DCM was added to the reaction mixture slowly over 15 min. After all of the DCC was added, the reaction mixture was left to stir at room temperature for 48 h. The reaction mixture was gravity filtered to remove the unreacted CPTP-DCC adduct and CPTP-An (in the filtrate) was further purified via flash chromatography (Biotage Isolera One with Luknova SuperSep silica prepacked columns) using a mixture of DCM and hexane (70:30 v/v; R_f = 0.45). The fractions collected were dried under vacuum in an oven (45 °C) for ≈12 h. The final product was a reddish-pink solid. ^{1}H NMR (400 MHz, $CDCl_3$, TMS): δ (ppm) = 8.53 (s, 1 H; CH), 8.34 (d, ^3J(H,H) = 8.9 Hz, 2 H; CH), 8.04 (d, ^3J(H, H) = 8.4 Hz, 2 H; CH), 7.86 (d, ^3J(H,H) = 8.2 Hz, 2 H; CH), 7.54 (m, 5 H; CH), 7.37 (t, ^3J(H,H) = 7.7 Hz, 2 H; CH), 6.22 (s, 2 H; CH_2), 2.68 (m, 2 H, CH_2), 2.46 (m, 2 H, CH_2), 1.87 (s, 3 H; CH_3). UV-vis (toluene): $\lambda_{max}(\epsilon)$ = 365 nm (8528 M^{-1} cm^{-1}).

Polymer Synthesis using RAFT Polymerization and CPTP-An as Chain Transfer Agent: A typical RAFT polymerization procedure for polymer synthesis using CPTP-An as chain transfer agent (CTA) was as follows: To a 50 mL Schlenk flask, CPTP-An (40 mg, 0.0848 mmol, 1 equiv.), MMA (849 mg, 0.903 mL, 8.48 mmol, 100 equiv.), AIBN (2.78 mg, 0.0170 mmol, 0.2 equiv.), toluene (5.65 mL), and a stir bar were added; the target MW was 10,000 g mol^{-1} (corresponding to a *DP* of 100). The reaction mixture was degassed through 3 cycles of freezing, vacuum pumping, and thawing to remove oxygen. The polymerization was conducted at 75 °C while stirring and aliquots were taken with a needle/syringe at various times ranging from 0 to 135 min. For each time interval study, a small amount of reaction solution was taken (≈1 mL) and then cooled down to room temperature with N_2 blowing over the solution's surface to concentrate it. Subsequently, the aliquots were dried overnight under vacuum in an oven at 55 °C. For the synthesis of PS and PMA, a similar polymerization procedure was performed while the reaction temperature was 100 °C for PS ($[S]_o$ = 1.5 and a target *DP* of 100) and 85 °C for PMA ($[MA]_o$ = 1.9 and a target *DP* of 125) and used the same procedure for taking aliquots.

Characterization: Nuclear magnetic resonance (NMR) spectroscopy was performed using a Bruker 400 MHz NMR with sample concentrations of ≈15 mg mL^{-1} in $CDCl_3$. ^{1}H NMR experiments for CPTP-An were performed with 32 proton scans and a proton relaxation decay of 5 s. ^{13}C NMR experiments for CPTP-An were done with 512 scans and a relaxation delay of 5 s. Baseline correction and analysis of the NMR spectra were performed using TopSpin 4.0.7. Electrospray ionization time-of-flight (ESI-TOF) mass spectrometry for CPTP-An was performed using an Agilent 6230 ESI-TOF. UV–vis absorption spectra of all samples were recorded at room temperature in toluene using a Thermo Scientific Genesys 30 visible spectrophotometer. Anthracene concentrations were calculated from absorbance values obtained from UV-vis spectroscopy with the Beer-Lambert law:

$$A = \epsilon bc \quad (2)$$

where *A* is the absorbance, ϵ is the molar absorptivity (unit: L mol^{-1} cm^{-1}), *b* is the path length of the sample (1 cm), and *c* is the concentration (unit: M).

For polymer samples, ^{1}H NMR experiments were performed with 32 proton scans and a proton relaxation decay of 3 s. Polymerization reaction conversions were calculated using the ratio of the *DP* calculated from NMR end-group analysis to the target *DP*. Gel permeation chromatography (GPC) measurements were performed for the polymers using a TOSOH EcoSEC HLC-8320 GPC with a TSKgel SuperMultiPore HZ-M. The instrument calibration was done with a series of PS standards (PStquick MP-M). All of the experiments were done at 40 °C. The mobile phase was HPLC grade THF using a flow rate of 1.0 mL min^{-1}. The sample concentrations were 2 mg mL^{-1} in THF with an injection volume of 10 µL.

Steady-state fluorescence measurements were performed with a PTI-Horiba QuantaMaster 400 spectrofluorometer equipped with a 75 W Xe arc lamp. Polymer sample concentrations were ≈1–3·10^{-6} M. These concentrations were sufficiently diluted to prevent intermolecular FRET from occurring. The critical overlap concentration c* for the random coil in a good solvent can be estimated using the following equation: c* = $M/N_A(R_{ee}/2)$,[3,54] in which N_A and *M* are Avogadro's number and polymer molecular weight, respectively. Using this equation, it can be estimated that the *c** for PS and PMMA (with *MW* up to 5,000 g mol^{-1}) studied in this work is in the range of 0.1–0.2 mg mL^{-1} (0.02–0.04 M for *MW* = 5,000 g mol^{-1}). Therefore, the experimental conditions are well below the critical overlapping concentration. For samples containing anthracene, an excitation wavelength of 365 nm and emission spectra were collected from 380 to 540 nm.

FRET Calculations: The Förster distance, R_o, is a characteristic distance for each specific FRET pair,[49] which is also the distance between the donor and acceptor when the FRET efficiency, E, is 50%. The Förster distance can be calculated using the following equation:

$$R_o = 0.211\left(\frac{\kappa^2 Q_D J(\lambda)}{\eta^4}\right)^{1/6} \quad (3)$$

where κ^2 is an orientation factor of the dipoles and is 0.67 for a freely rotating donor and acceptor (in solution state), Q_D is the fluorescence quantum yield of the acceptor of the donor ($Q_D = 0.29$ for An), $J(\lambda)$ is the area integral of the spectral overlap between the molar-normalized donor emission and the acceptor absorption spectra, and η is the refractive index of the medium ($\eta = 1.49$ for toluene). To determine $J(\lambda)$, the following equation can be used:

$$J(\lambda) = \frac{\int_0^\infty F_D(\lambda)\,\epsilon_A(\lambda)\,\lambda^4 d\lambda}{\int_0^\infty F_D(\lambda)\,d\lambda} \quad (4)$$

where ϵ_A is the extinction coefficient of the acceptor (in M^{-1} cm^{-1}), λ is the wavelength in the unit of nm, and F_D is the wavelength dependent donor fluorescence emission spectrum normalized to an area of 1. For this FRET pair (anthracene and CPTP), the spectral overlap was determined to be $1.19 \cdot 10^{13}$ M^{-1} cm^{-1} nm.[4]

To measure the distance of FRET donor and acceptor pair, the emission intensity was measured over 380–540 nm using an excitation wavelength of 365 nm. The emission intensities were normalized with the molar concentration of anthracene molecules measured by UV-vis spectroscopy. The FRET efficiency can then be calculated using the following equation:

$$E = \frac{1}{1 + (r/R_o)^6} = 1 - \frac{I_{DA}}{I_D} \quad (5)$$

where I_{DA} and I_D are the total donor fluorescence emission intensity (molar concentration normalized) in the presence and absence of the acceptor, respectively, and r is the distance between the donor and acceptor.

Once the FRET efficiency has been measured, the distance (R_{ee}) between the donor and acceptor, located on respective polymer chain ends, can be calculated using the following equation:

$$E = \int_{R_{ee,\,min}}^{R_{ee,\,max}} p(R_{ee})\,\frac{R_o^6}{R_o^6 + R_{ee}^6}\,dR_{ee} \quad (6)$$

where R_{ee} is the average end-to-end distance of the polymer chains and $p(R_{ee})$ follows the flexible chain model with the equation described as below:

$$p(R_{ee}) = 4\pi r^2\left(\frac{3}{2\pi N b^2}\right)^{3/2} exp\left(-\frac{3}{2}\frac{R_{ee}^2}{N b^2}\right) \quad (7)$$

where N is the total amount of chain segments and b is the Kuhn length of the polymer.

Supporting Information

Supporting Information is available from the Wiley Online Library or from the author.

Acknowledgements

This work was partially supported by the National Science Foundation Office of Integrative Activities #2132144. SI acknowledges the support by the National Science Foundation REU program (#1950387). ZQ and SV acknowledge the financial support provided from the ACS Petroleum Research Fund (award no. 65268-DNI7). The author would also like Penelope Jankoski for her support in performing mass spectrometry experiments at the University of Southern Mississippi Facility.

Conflict of Interest

The authors declare no conflict of interest.

Data Availability Statement

The data that support the findings of this study are available from the corresponding author upon reasonable request.

Keywords

fluorescence, in-situ characterization, polymer conformation

Received: August 1, 2024
Revised: September 16, 2024
Published online: September 23, 2024

[1] P. C. Heimenz, T. P. Lodge, *Polymer Chemistry*, CRC Press, Boca Raton, FL, **2007**.
[2] Z. G. Wang, *Macromolecules* **2017**, *50*, 9073.
[3] S. Chandran, J. Baschnagel, D. Cangialosi, K. Fukao, E. Glynos, L. M. C. Janssen, M. Müller, M. Muthukumar, U. Steiner, J. Xu, S. Napolitano, G. Reiter, *Macromolecules* **2019**, *52*, 7146.
[4] V. Abetz, K. Kremer, M. Müller, G. Reiter, *Macromol. Chem. Phys.* **2019**, *220*, 1800334.
[5] S. Askar, C. M. Evans, J. M. Torkelson, *Polymer* **2015**, *76*, 113.
[6] S. Chandran, G. Reiter, *ACS Macro Lett.* **2019**, *8*, 646.
[7] A. P. Marencic, R. A. Register, *Annu. Rev. Chem. Biomol. Eng.* **2010**, *1*, 277.
[8] L. Liu, M. Zhu, X. Xu, X. Li, Z. Ma, Z. Jiang, A. Pich, H. Wang, P. Song, *Adv. Mater.* **2021**, *33*, 2105829.
[9] G. Lu, S. Lu, J. Sun, M. W. Boey, W. Shang, J. Wu, A. K. An, *Adv. Funct. Mater.* **2024**, *34*, 2309913.
[10] M. Guo, Z. Qu, F. Min, Z. Li, Y. Qiao, Y. Song, *InfoMat* **2022**, *4*, e12323.
[11] S. K. Brar, M. Verma, *TrAC, Trends Anal. Chem.* **2011**, *30*, 4.
[12] B. Chu, B. S. Hsiao, *Chem. Rev.* **2001**, *101*, 1727.
[13] J. J. Kwok, K. S. Park, B. B. Patel, R. Dilmurat, D. Beljonne, X. Zuo, B. Lee, Y. Diao, *Macromolecules* **2022**, *55*, 4353.
[14] Y. Wang, W. Wang, K. Hong, C. Do, W. R. Chen, *Polymer* **2020**, *204*, 122698.
[15] S. P. O. Danielsen, C. R. Bridges, R. A. Segalman, *Macromolecules* **2022**, *55*, 437.
[16] Y. Wei, M. J. A. Hore, *J. Appl. Phys.* **2021**, *129*, 171101.
[17] L. H. Sperling, *Polym. Eng. Sci.* **1984**, *24*, 1.
[18] N. Sherck, T. Webber, D. R. Brown, T. Keller, M. Barry, A. Destefano, S. Jiao, R. A. Segalman, G. H. Fredrickson, M. S. Shell, S. Han, *J. Am. Chem. Soc.* **2020**, *142*, 19631.
[19] G. Jeschke, *Annu. Rev. Phys. Chem.* **2012**, *63*, 419.
[20] J. E. Banham, C. M. Baker, S. Ceola, I. J. Day, G. H. Grant, E. J. J. Groenen, C. T. Rodgers, G. Jeschke, C. R. Timmel, *J. Magn. Reson.* **2008**, *191*, 202.
[21] P. Rajdev, S. Ghosh, *J. Phys. Chem. B* **2019**, *123*, 327.
[22] S. Valdez, M. Robertson, Z. Qiang, *Macromol. Rapid Commun.* **2022**, *43*, 2200421.

[23] K. Truong, M. Ikura, *Curr. Opin. Struct. Biol.* **2001**, *11*, 573.
[24] H. Mazal, G. Haran, *Curr. Opin. Biomed. Eng.* **2019**, *12*, 8.
[25] T. Heyduk, *Curr. Opin. Biotechnol.* **2002**, *13*, 292.
[26] Z. H. Mohamed, C. Rhein, E. M. Saied, J. Kornhuber, C. Arenz, *Chem. Phys. Lipids* **2018**, *216*, 152.
[27] S. R. Alam, H. Wallrabe, Z. Svindrych, A. K. Chaudhary, K. G. Christopher, D. Chandra, A. Periasamy, *Sci. Rep.* **2017**, *7*, 10451.
[28] H. J. Chial, P. Lenart, Y. Q. Chen, *PLoS One* **2010**, *5*, e12471.
[29] Y. Ma, Y. Yamamoto, P. R. Nicovich, J. Goyette, J. Rossy, J. J. Gooding, K. Gaus, *Nat. Biotechnol.* **2017**, *35*, 363.
[30] C. King, V. Raicu, K. Hristova, *J. Biol. Chem.* **2017**, *292*, 5291.
[31] S. W. A. Reulen, M. Merkx, *Bioconjugate Chem.* **2010**, *21*, 860.
[32] X. Sun, G. Wang, H. Zhang, S. Hu, X. Liu, J. Tang, Y. Shen, *ACS Nano* **2018**, *12*, 6179.
[33] A. Watanabe, M. Matsuda, *Macromolecules* **1986**, *19*, 2253.
[34] M. Zammarano, P. H. Maupin, L. P. Sung, J. W. Gilman, E. D. McCarthy, Y. S. Kim, D. M. Fox, *ACS Nano* **2011**, *5*, 3391.
[35] W. Meesorn, A. Shirole, D. Vanhecke, L. M. De Espinosa, C. Weder, *Macromolecules* **2017**, *50*, 2364.
[36] H. Wahdat, M. Gerst, S. Möbius, J. Adams, *J. Appl. Polym. Sci.* **2020**, *137*, 48972.
[37] Q. A. Besford, H. Yong, H. Merlitz, A. J. Christofferson, J. U. Sommer, P. Uhlmann, A. Fery, *Angew. Chem., Int. Ed.* **2021**, *60*, 16600.
[38] N. Y. Chan, M. Chen, X. T. Hao, T. A. Smith, D. E. Dunstan, *J. Phys. Chem. Lett.* **2010**, *1*, 1912.
[39] L. Qin, L. Li, Y. Sha, Z. Wang, D. Zhou, W. Chen, G. Xue, *Polymers* **2018**, *10*, 1007.
[40] Y. Sha, Y. Xu, D. Qi, Y. Wan, L. Li, H. Li, X. Wang, G. Xue, D. Zhou, *Macromolecules* **2016**, *49*, 8274.
[41] Y. Sha, D. Qi, S. Luo, X. Sun, X. Wang, G. Xue, D. Zhou, *Macromol. Rapid Commun.* **2017**, *38*, 1600568.
[42] L. Qin, N. Zhao, Y. Sha, H. Chen, L. Li, D. Zhou, W. Chen, G. Xue, X. Jia, *Polymer* **2020**, *190*, 122217.
[43] C. J. Ellison, J. M. Torkelson, *Nat. Mater.* **2003**, *2*, 695.
[44] D. J. Mai, C. M. Schroeder, *ACS Macro Lett.* **2020**, *9*, 1332.
[45] Z. Qiang, M. Wang, *ACS Macro Lett.* **2020**, *9*, 1342.
[46] A. A. Karanastasis, G. S. Kenath, R. Sundararaman, C. K. Ullal, *Soft Matter* **2019**, *15*, 9336.
[47] K. Skrabania, A. Miasnikova, A. M. Bivigou-Koumba, D. Zehm, A. Laschewsky, *Polym. Chem.* **2011**, *2*, 2074.
[48] N. Zhou, L. Lu, X. Zhu, X. Yang, X. Wang, J. Zhu, D. Zhou, *Polym. Bull.* **2006**, *57*, 491.
[49] I. Medintz, N. Hildebrandt, *FRET – Forster Resonance Energy Transfer*, Wiley, Hoboken, NJ **2013**.
[50] H. Tobita, *Macromol. React. Eng.* **2008**, *2*, 371.
[51] W. A. Braunecker, K. Matyjaszewski, *Prog. Polym. Sci.* **2007**, *32*, 93.
[52] S. I. Rosenbloom, R. J. Sifri, B. P. Fors, *Polym. Chem.* **2021**, *12*, 4910.
[53] Y. Wang, A. W. Fortenberry, W. Zhang, Y. C. Simon, Z. Qiang, *J. Phys. Chem. B* **2023**, *127*, 3100.
[54] Q. Yingt, B. Chu, *Macromolecules* **1987**, *20*, 362.